

# Histone modifications form a cell type specific chromosomal bar

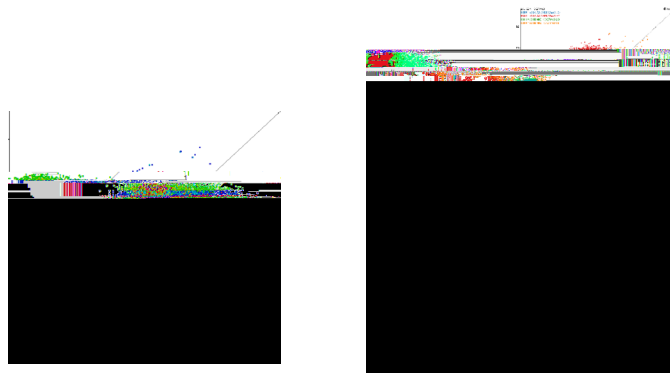
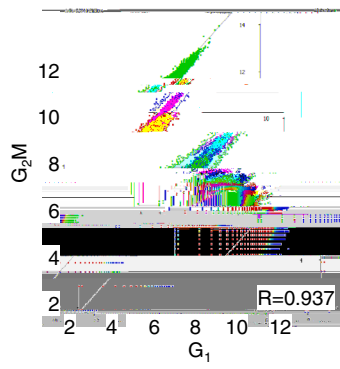


## Bands of histone PTM detected by immunofluorescence microscopy on metaphase chromo

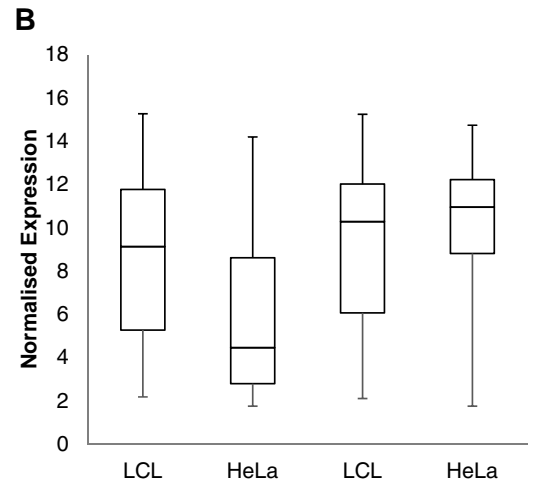
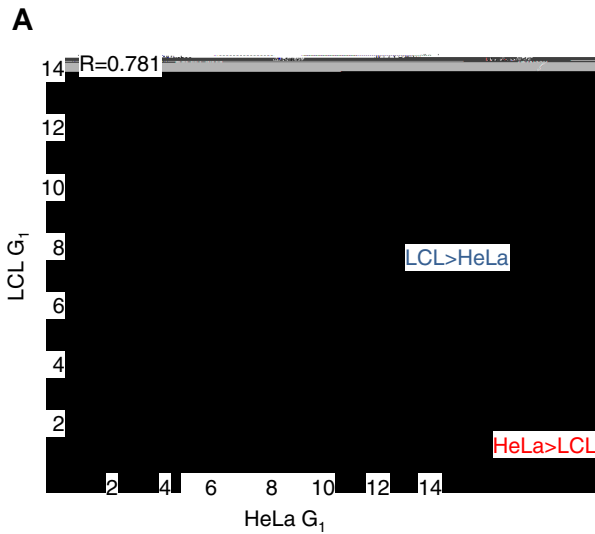
## B H3K9ac in LCL and HeLa

6

low in H3K27me3 (10,156 genes) and those low in H3K4me3 and high in H3K27me3 (8315 genes). In these differentiated cells only a small proportion of genes (2825 genes) were present in bivalent domains, relatively highly enriched in both marks. This pattern was consistent between cell cycle phases and TSS retained their position in the distribution from G<sub>1</sub> to G<sub>2</sub>M (Fig. 2D, insets). Expression levels from genes in each population were determined by microarray from asynchronous cells (Fig. 2E). Functional enrichment of genes from each quadrant is summarised in Supplementary figure S8. As might be expected, expression was highest from TSS with

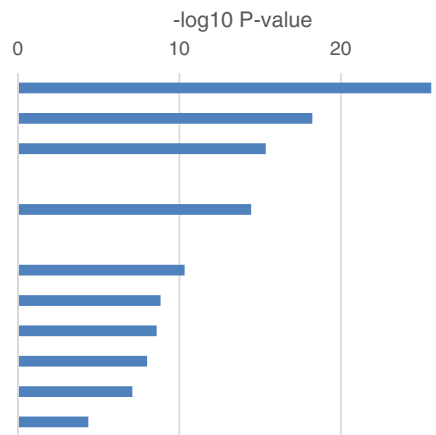


high H3K4me3 and low H3K27me3 and this group was modestly enriched in genes involved in housekeeping processes such as mitochondria (fold enrichment (FE) 1.7,  $P = 2.5 \times 10^{-18}$ ), ribonucleoprotein complex (FE 1.9,  $P = 9.6 \times 10^{-14}$ ) and RNA processing (FE 1.7,  $P = 1.6 \times 10^{-9}$ ). Expression was lowest from TSS with high H3K27me3 and low H3K4me3 and these genes were enriched in cell-type specific genes which would not be expected to be expressed in LCLs such as epidermis development (FE 2.2,  $P = 8.5 \times 10^{-8}$ ), neurological system process (FE 1.5,  $P = 2.7 \times 10^{-12}$ ) and embryonic organ morphogenesis (FE 2.1,  $P = 1.2 \times 10^{-5}$ )



**LCL > HeLa**

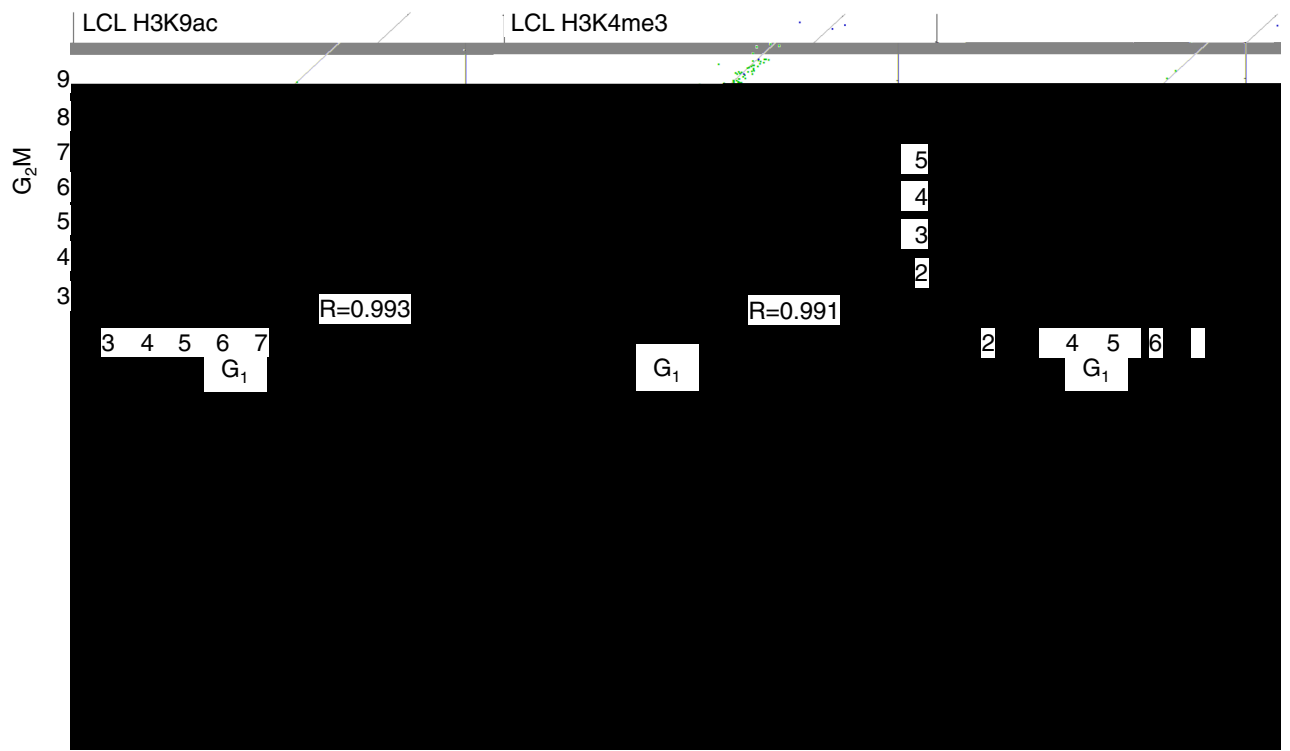
	C	%	FE
Q:0005622	230	13.1	2.0
Q:0005886	497	28.4	1.4
Q:0003700	158	9.0	1.9
Q:0050853	28	1.6	6.0
Q:0003676	145	8.3	1.7
Q:0006955	76	4.3	2.1
Q:0045211	47	2.7	2.6
Q:0002250	37	2.1	2.9
Q:0006954	66	3.8	2.0
Q:0042613	10	0.6	5.3



**HeLa > LCL**

	C	%	FE
Q:0005515	2395	55.8	1.2
Q:0005829	1053	24.5	1.5
Q:0005654	889	20.7	1.5
Q:0016020	656	15.3	1.4
Q:0005524	486	11.3	1.4
Q:0005913	143	3.3	2.0
Q:0098641	133	3.1	2.0
Q:0005813	166	3.9	1.8

Despite the strong correlations shown by these scatter plots, there are outliers towards the edges of the distributions (Fig. 5). We asked whether these have any functional significance, perhaps representing distinct









close correlation was found when different cell cycle phases were compared (R values between 0.91 and 0.98 for all three modifications). When the same procedure was used to compare H3K9ac at equivalent cell cycle phases in HeLa and LCL, the correlation, though still present, was much lower (R = 0.78). Further, outlying regions on either the LCL or HeLa sides of the distribution, were enriched in genes likely to be preferentially expressed in either HeLa or LCL, i.e. cell-type-specific genes. These results are consistent with the proposition that variation in PTM distribution at 1–2 Mb and below reflects the distinctive patterns of transcription, or transcriptional potential, that characterize the two cell types, LCL and HeLa.







cycle of the genomic distribution of histone PTM, specifically H3K9ac, H3K4me3 and H3K27me3, indicates their close involvement in this process.

### Conclusions

Genome-wide analysis by ChIP-seq, shows histone modifications H3K4me3, H3K9ac and H3K27me3 to be relatively enriched over chromosomal domains of 10–50 Mb. These domains do not differ detectably between cell types, do not vary through the cell cycle and correspond to bands detectable by immunofluorescence microscopy of metaphase chromosome spreads. The relatively high levels of both activating and silencing histone PTM in these regions are likely to be by-products of their high gene density.

in digestion buffer (0.32 M sucrose, 50 mM Tris/HCl (pH7.4), 4 mM





57. Hansen, A. S., Cattoglio, C., Darzacq, X. & Tjian, R. Recent evidence that TADs and chromatin loops are dynamic structures. *Nucleus*. **1**, 20–32 (2018).
58. Gibcus, J. H. *et al.* A pathway for mitotic chromosome formation. *Science* **359**, 1–10 (2018).
59. Turner, B. M. Cellular memory and the histone code. *Cell* **1**, 285–291 (2002).
60. Halsall, J., Gupta, V., O'Neill, L. P., Turner, B. M. & Nightingale, K. P. Genes are often sheltered from the global histone hyperacetylation induced by HDAC inhibitors. *PLoS ONE* **7**, e33453 (2012).
61. Halsall, J. A., Turan, N., Wiersma, M. & Turner, B. M. Cells adapt to the epigenomic disruption caused by histone deacetylase inhibitors through a coordinated, chromatin-mediated transcriptional response. *Epigenet. Chrom.* **8**, 29 (2015).
62. Peart, M. J. *et al.*

